Received: 13 October 2021 | Accepted: 30 November 2021

DOI: 10.1002/pip.3526

RESEARCH ARTICLE

PROGRESS IN PHOTOVOLTAICS WILEY

High time resolution measurement of solar irradiance onto driving car body for vehicle integrated photovoltaics

Gustav Wetzel[1] | Leon Salomon[1] | Jan Krügener[1] | Dennis Bredemeier[2,3] | Robby Peibst[1,3]

[1]Institute of Electronic Materials and Devices Leibniz University Hannover, Hannover, Germany

[2]Department of Solar Energy, Institute of Solid-State Physics, Leibniz University Hannover, Hannover, Germany

[3]Institute for Solar Energy Research Hamelin, Emmerthal, Germany

Correspondence
Gustav Wetzel, Institute of Electronic Materials and Devices Leibniz University Hannover, Schneiderberg 32, 30167, Hannover, Germany.
Email: wetzel@mbe.uni-hannover.de

Funding information
Bundesministerium für Wirtschaft und Energie; German Federal Ministry for Economic Affairs and Energy (BMWi), Grant/Award Number: 0324275F

Abstract

Vehicle integrated photovoltaic (VIPV) systems have much different requirements on maximum power tracking compared to stationary setups. The occurrence of fast changes between full irradiance and shading are demanding. To evaluate the specific impact of these conditions on the specifications of VIPV systems, we conduct high resolution measurements of the incident irradiance onto a car body while driving. We investigate the influence of environmental conditions like weather, season and building density in an urban environment on measured irradiance on the roof and the sides of a vehicle. We find that weather conditions have the highest impact on the measured irradiance on the roof, while the relative irradiance on the side depends more heavily on the season. We also find that changes in irradiance occur predominantly at frequencies below 1 Hz, but changes with 100 Hz or more can occur in certain situations, with a tendency toward higher frequencies for sunny weather. This must be considered in maximum power point tracker design.

KEYWORDS

electric vehicle, solar powered, transient illumination, transient shading, VIPV

1 | INTRODUCTION

The electrification of automobiles is a promising attempt to reduce CO_2 emissions from personal and goods transport, as electric vehicles can run on renewable energy and can even contribute to grid regulation.[1–3] Vehicle Integrated Photovoltaics (VIPV) has the potential to increase the range and thus to reduce the number of required charging events from the grid.[4,5] It can deliver additional power for driving as well as for other loads such as air conditioning or infotainment, so the battery is less utilized. Compared to passenger cars, delivery vehicles provide relatively large flat roof and side areas which favor the integration of PV-modules. The integration into vehicles comes with various new challenges to PV-system design though.[6,7]

A challenge rarely studied so far is transient illumination which can occur at significantly higher frequencies compared to stationary use. A maximum power point tracker (MPPT) for VIPV potentially has to handle fast changes in the output power of the solar cells. In this work we therefore investigate with high resolution the transient irradiance on different sides of a vehicle while driving for different environmental conditions, for example, season, clouding, foliation and street types. With the results of our experiment we can give an assessment of the switching requirements on MPPTs for use in VIPV.

2 | TEST SETUP AND TEST ROUTE

The test setup we use was presented in Wetzel et al.[8] To measure the solar irradiance on the roof and the side of a vehicle while driving, we attach three Kipp & Zonen SP2 Lite 2 pyranometers on a van with a modified roof rack. The used pyranometers are silicon based and have a spectral range of 400 to 1100 nm and a response time lower than 500 ns. One is oriented toward the left side with respect to the direction of driving, one to the right side and one upward. The output signal is an analogue voltage, which is proportional to the solar irradiance on the sensor with a sensitivity of 72 μ V/W/m^2 and is recorded by a digital oscilloscope with a sampling rate of 1000 samples per second. We use GPS to track the location and speed with a sampling rate of 1 sample per second. Additionally there is an upward-looking video camera installed on the roof rack for monitoring the environment and helping with correlation of the oscilloscope data with the driving situation. A picture of the test setup is shown in Figure 1.

We use the same test route of about 21-km length as presented in Wetzel et al,[8] located in Hannover, Germany (52°22'28" N 9°44'19"E), for all our test runs. It features several sections that represent different situations that can typically occur while driving in an urban environment. The sections are grouped in three different categories: The first is "narrow streets" with a low speed limit of 30 km/h and a high building density. The building height is mostly higher than the distance between vehicle and building. The second is "wide streets slow" with a speed limit of 50 km/h. These are streets like alleys and streets with more than one lane per direction. The distance from the vehicle to buildings is usually higher than the building height. The average building height in the vicinity of "narrow streets" and "wide streets slow" is 15 m with a standard deviation of 6.5 m, according to digital 3D building data.[9] The last is "wide streets fast" with a speed limit of 80 km/h. This is a city highway with no buildings in the vicinity that cast shadows on the street, but with several overpasses. The route was also chosen so there were about equally long sections in predominantly north-south (or south-north) direction as in predominantly east-west (or west-east) direction for every category. The route is depicted in the satellite image in Figure 2, each test run takes about 40 to 55 min per trip depending on traffic.

The data used in this work was obtained in six test runs, that took place in the period between autumn 2019 and summer 2020 (due to the COVID-19 situation, there were no test runs possible in spring). Table 1 shows the date, time and the weather conditions for the test runs, as well as the solar angles and the global and diffuse solar radiation measured at the Institute of Meteorology and Climatology of the Leibniz University Hannover, which is located close to the test route.[11] We conducted two test runs for each season, one under cloudy and one under sunny conditions, within short time interval (1 to 6 days) for comparable solar angles. The main difference is the

FIGURE 1 Picture of the test setup with three pyranometers mounted on the car roof. With one pyranometer looking upward and one looking to the left and to the right side each

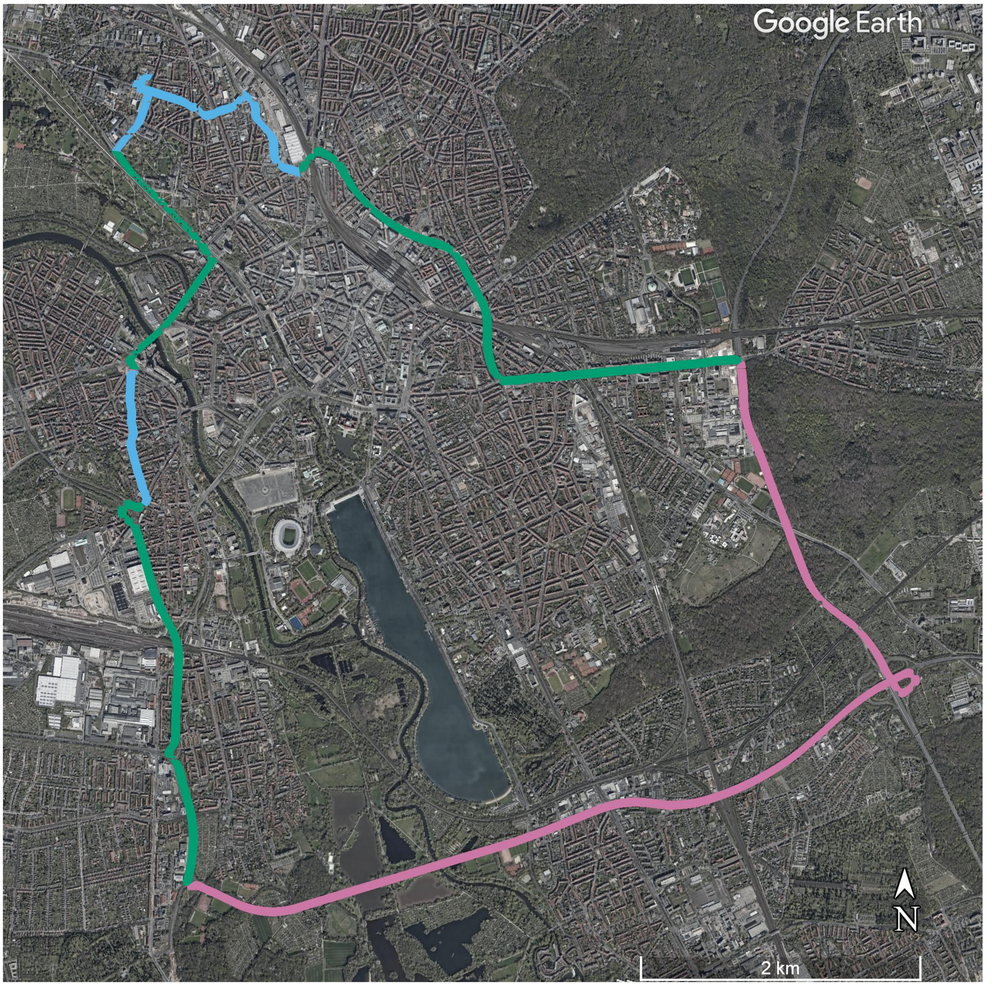

FIGURE 2 The GPS track of the test route. The direction of driving is counter clockwise with the start/end-point in the north west. The blue parts of the track indicate “narrow streets” with a speed limit of 30 km/h, the green parts indicate “wide streets slow” with a speed limit of 50 km/h and the pink part indicates “wide streets fast” with a speed limit of 80 km/h[10]

TABLE 1 Overview of the conducted test runs with, date, time, and weather conditions

Run	Season	Date	Time (UTC)	Solar zenith angle[12]	Solar azimuth angle[12]	Weather	Average global radiation[11]	Average diffuse radiation[11]
1	Autumn	September 3, 2019	11:02–11:51	45.05°–44.76°	173.50°–190.67°	Cloudy	311 W/m^2	303 W/m^2
2	Autumn	September 5, 2019	11:21–12:14	44.47°–43.12°	180.40°–198.57°	Sunny	388 W/m^2	225 W/m^2
3	Winter	February 27, 2020	12:56–13:36	26.74°–23.88°	202.87°–213.34°	Cloudy	147 W/m^2	147 W/m^2
4	Winter	February 28, 2020	8:18–9:05	16.63°–21.75°	128.87°–139.92°	Sunny	306 W/m^2	79 W/m^2
5	Summer	June 18, 2020	11:04–11:59	60.84°–60.22°	171.36°–197.12°	Cloudy	154 W/m^2	154 W/m^2
6	Summer	June 24, 2020	11:11–11:54	60.93°–60.45°	174.04°–194.24°	Sunny	885 W/m^2	72 W/m^2

Note: The global and diffuse radiation values where measured at the Institute of Meteorology and Climatology of the Leibniz University Hannover, which is located close to the test route.

higher ratio of diffuse light on the respective cloudy day compared to the sunny one. An example of the different situations can be seen in Figure 3 which shows a snapshots from the recorded video data taken at the same location on September 3, 2019 (cloudy) and September 5, 2019 (sunny), respectively. The main difference between seasons is the solar altitude, but in winter the lack of foliation is also a factor that can affect the incident irradiance on the car, as can be seen in Figure 4.

3 | MEASURED SOLAR IRRADIANCE ON CAR BODY

3.1 | Irradiance incident on the roof

Figure 5A shows the average measured irradiance on the roof of the car with respect to the different street categories and seasons; Figure 5B shows the deviation of the measured irradiance for the

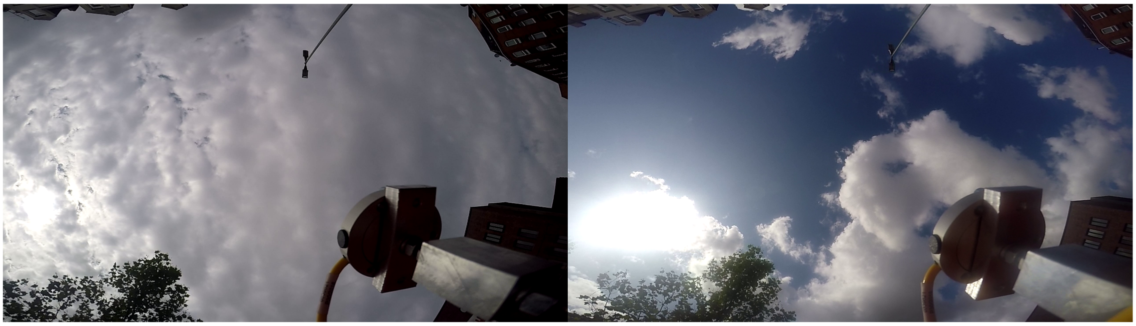

FIGURE 3 Snapshots of the recorded video data at the same location on the test route at the cloudy day (left) and sunny day (right). In the bottom right hand corner of the pictures you can see the upward-looking pyranometer on the car roof. The direction of driving is from the right to the left

FIGURE 4 Snapshots at the same location of the test route in winter (left) and summer (right). The lack of foliation in winter can have a significant effect on the incident irradiance on the car when driving on a street with lots of trees in the vicinity, like alleys

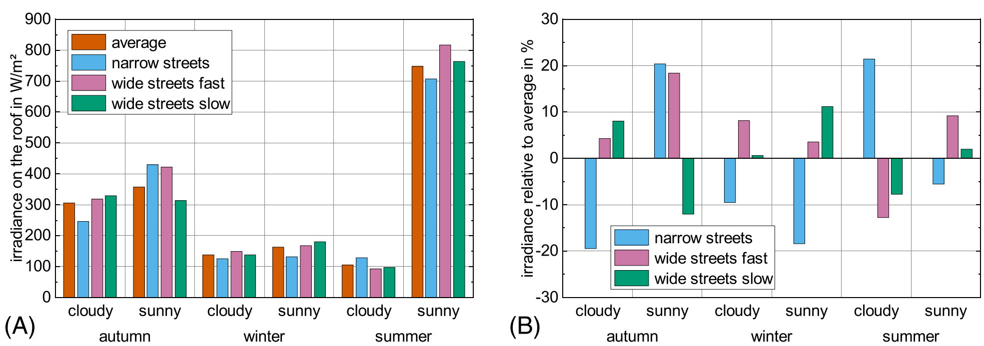

FIGURE 5 (A) The measured irradiance on the car roof for six different test runs in autumn, winter, and summer. One with cloudy and one with sunny weather for each season. Shown is the overall measured average irradiance and the average irradiance measured on the different street types. (B) The relative irradiance for the different street types compared to the average irradiance measured for the respective test run. The influence of the street types is comparably small, while the season affect the incident irradiance more. The weather conditions have an even higher influence especially in summer. The influence of the street types varies heavily with the season and weather conditions. No clear trends can be found here

different street types from the average irradiance on the respective test run. As one would expect the irradiance is always higher for the respective sunny days. The difference to cloudy conditions though depends heavily on the season. In winter there is barely any difference between the two test runs while in summer the average irradiance under sunny conditions is almost eight times higher as when cloudy. The solar altitude (see Table 1) is significantly lower in winter, so the amount of direct irradiance incident on the roof is comparably low. Therefore at cloudy conditions, due to increased scattering in the atmosphere, the amount of diffuse light is higher, so that it compensates partially the decreased direct light. In summer, due to the substantially higher solar altitude, the amount of direct light is so high at sunny conditions, that the increased amount of diffuse light when cloudy cannot compensate that. Also the average irradiance on the cloudy day in summer is the lowest measured in all test runs. The cloud density is apparently more crucial for the incident irradiance than the solar altitude. Thus the weather conditions can have an even higher effect on the irradiance than the season. Even though the average irradiance is higher for the sunny days, that does not apply to all sections of the test route. We will further investigate the influence of different ambient situations, regarding the street categories described in Section 2 below.

The time averaged irradiance in autumn is 305 W/m^2 for the cloudy day and 357 W/m^2 for the sunny day (see Figure 5). For "wide streets slow" the average irradiance is even slightly lower on the sunny day (318 W/m^2 vs. 329 W/m^2 when cloudy). The reason for that is likely the occurrence of cumulus clouds during the second half of the run (including the larger part of that category), which temporarily cause a more intense shadowing as the more high fog like clouding on the other run. That also results in the fact that, on the sunny day, the average irradiance in category "wide streets slow" is significantly lower than in category "narrow streets" (429 W/m^2) and "wide streets fast" (422 W/m^2), while for the cloudy day the category "narrow streets" shows the lowest average irradiance (245 W/m^2), and "wide streets fast" (318 W/m^2) is very close to "wide streets slow". Due to the higher building density around "narrow streets" and the closer distance of the buildings to the street, it is more likely, that the sun is obscured by objects than for wider streets.[13,14] Therefore, one would expect the measured irradiance to be lower here, as it is found for the majority of the measurements. Because of the lower amount of direct light and more diffuse light one would expect this to be less significant for cloudy conditions. Apparently the opposite is the case in autumn. An explanation for this behavior might be reflections on buildings on the other side of the street. The probability that light reflected by buildings is incident on the car depends on the relation between solar altitude, the height and albedo of the building and the distance from the car to the building. For the autumn test runs the solar altitude is moderate with about 45°, while it is substantially lower in winter and higher in summer. So this effect does not occur for the other seasons.

In winter the overall irradiance is significantly lower, and the ratio of the time averaged irradiance between cloudy (138 W/m^2) and sunny weather (162 W/m^2) is almost identical. For the cloudy day the street types have little influence on the measured irradiance compared with the autumn measurements, for the sunny day "narrow streets" show a significantly lower irradiance, what would correspond to the shading effects by buildings discussed above.

In summer there is a considerably higher difference between sunny and cloudy conditions as the average irradiance on the sunny day (748 W/m^2) is more than seven time higher than on the cloudy day (105 W/m^2). The influence of the street type is comparably marginal here for the sunny day. Remarkable is that the irradiance on "narrow streets" is 21% higher than average for cloudy conditions. This is the highest deviation due to street type we found. In this case the only plausible explanation is a change of the cloud density during the test runs, what lead to higher overall irradiance on the "narrow streets" sections. Due to the low overall irradiance on this test run, the relative deviation corresponds to only 23 W/m^2 absolute difference.

3.2 | Side-to-roof ratio

The average irradiance on the roof sensor reaches 2.38 times of the average irradiance on the side sensors (mean of left and right sensor). That is similar to the results obtained by Araki *et al.* in a stationary setup.[13] From this follows that on average 54.3% of the overall measured solar energy on the car is incident on the roof and 45.7% distributed to both sides. This ratio only marginally differs for most of the different runs when looking at the average of all street types, except for the sunny days in winter and in summer. Figure 6 shows the irradiance on the side-looking sensors (mean of the left and right sensor) relative to the measured irradiance on the roof sensor. On the sunny day in winter the irradiance measured on the sides can reach almost the values measured on the roof (67% to 93% depending on the street type). This is because of the low solar altitude (about 16° to 22°), which is more favorable for the vertical surfaces. Under these conditions, the maximum measured irradiance on the sides is almost twice as high as on the roof (998 W/m^2 vs. 534 W/m^2), what is even higher than the maximum value taken from stationary measurements in the area.[11] This is likely due to reflections which can increase the incident irradiance on the car temporarily. The reason the average irradiance is still lower than on the roof, is because the sides are more likely to be shaded by buildings[13] and also because only one side can face the sun directly at one time. On the sunny day in summer the

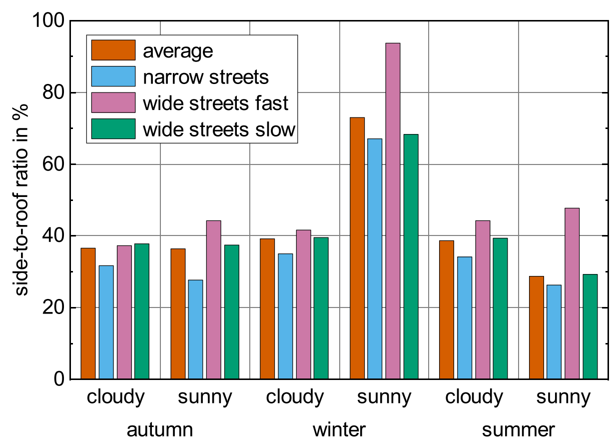

FIGURE 6 The amount of the measured irradiance on the car sides in ratio to the irradiance on the roof. The average side-to-roof ratio is 43.1%. For most of the test runs it differs only slightly. Only for the sunny day in winter it is substantially higher for all street types. For the sunny day in summer it is noticeably lower for the larger part of the test run, but higher for the "wide streets slow" section. The influence of the different street types is small compared to that of the weather conditions and different seasons

average irradiance on the sides is noticeably lower than the overall average. This can also be explained by the solar altitude, which is about 60° here and so favors horizontal surfaces. The higher ratio of diffuse light on the cloudy day does apparently lead to a higher side-to-roof ratio. Due to increased scattering in the cloud cover, the light can reach planes not directly facing the sun or planes that are obscured by buildings, trees, and so on, more easily. In autumn though, the weather conditions barely affect the overall side-to-roof ratio. The solar altitude is about 45° here so the irradiance onto vertical and horizontal surfaces is equivalently high. So the less direct and more diffuse light at cloudy conditions affect both roof and sides equally.

As stated earlier the average irradiance on the roof is much higher than on the sides for most of the test runs. The side-to-roof ratio during a test run also depends on the street type though. Therefore we take a closer look at the side to roof ratio with respect to the different street categories. Expectedly for all test runs the side-to-roof ratio is lowest for “narrow streets”. The higher the building density the more likely the sides are shaded. The wider the street, the lower is the probability that the side sensors are shaded by objects, so the side-to-roof ratio is consistently higher here. For almost all measurements “wide streets fast” shows the highest side-to-roof ratio, except for the cloudy day in autumn where the value for “wide streets slow” is marginally higher. The difference between the two wider street types is consistently higher for the sunny days. This is likely due to the more direct light. For the “wide streets fast” sections there are fewer buildings or other high objects in the vicinity that cast shadows than for the “wide streets slow” sections. For cloudy weather though, this becomes less significant due to the more diffuse light.

4 | FREQUENCY ANALYSIS OF THE MEASURED IRRADIANCE

The collected data provides information not only about the overall solar irradiance on the car, but the high sample rate also allows an analysis of the transient behavior of illumination while driving. In practice this can be relevant for MPPT design, as power changes might occur faster than the MPPT can handle them. That means that, for example shortly after a fast transition from very high to very low irradiance, the MPPT would not adjust the operating point of the PV-module fast enough, so the energy conversion efficiency would be reduced. Below we will discuss the frequency distribution of the occurring irradiance changes. Figure 7A shows an exemplary 10 min extract of the measured irradiance on the roof of the vehicle over time from the two runs in autumn. It is apparent that the amplitude of the irradiance is substantially higher for the sunny day. This is mostly due to the much higher maximum irradiance, and also the minimum irradiance is lower. As the the solar altitude is very similar for both test runs, this is likely due to the weaker diffuse light. Note that due to different traffic situations both signals are not exactly synchronous for the two runs. Figure 7B shows a 20 s extract at a cloverleaf interchange on the city highway with the measured irradiance from all three sensors. It is evident that irradiance changes from almost 1 sun to nearly zero or vice versa can occur within a sub-second time interval.

A fast Fourier transform (FFT) was performed on the recorded data. The FFT converts a waveform from time domain to frequency domain. Here, we use it to analyze the frequency spectrum at which illumination changes occur. The results for the two test runs in autumn are illustrated in Figure 8 exemplarily. It shows a continuous decrease in amplitude with increasing frequency for both cloudy and sunny conditions. On the cloudy day the decrease is much steeper though, while higher frequencies stay more prominent on the sunny day. This can be explained by more direct light on the sunny day which causes more hard edge shadows which in turn cause more abrupt dark-light or light-dark transitions and therefore a higher ratio of higher frequencies in the measured signal, while on the cloudy day the higher ratio of diffuse light causes more soft shadows and therefore smoother dark-light/light-dark transitions. The most relevant frequency range is below 1 Hz for both days, while higher frequencies contribute very little to the overall irradiance.

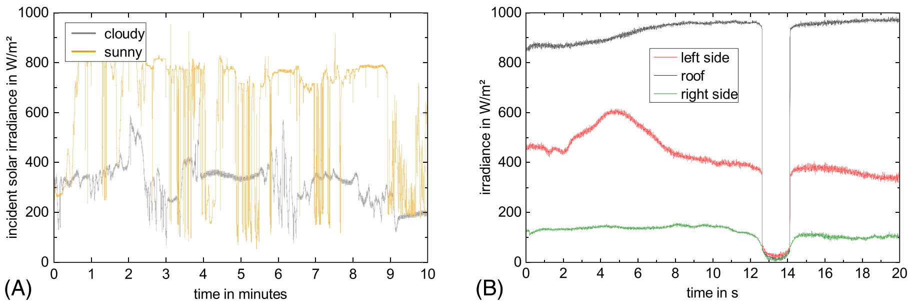

FIGURE 7 (A) The plot shows a 10-min extract of the measured irradiance on the roof of the vehicle over time from the two runs in autumn. The extract is from a “wide streets slow” section of the route, with the same starting point for both runs. Note that due to different traffic situations both signals are not exactly synchronous for the two runs. The irradiance amplitude is apparently much higher on the sunny day. (B) The plot shows a 20-s extract of the measured irradiance from all three sensors at a cloverleaf interchange on the city highway. The prominent drop in irradiance between 12 and 14 s is caused while passing under a bridge on the highway. It shows a change in irradiance of almost 1000 W/m^2 within time interval significantly shorter than a second

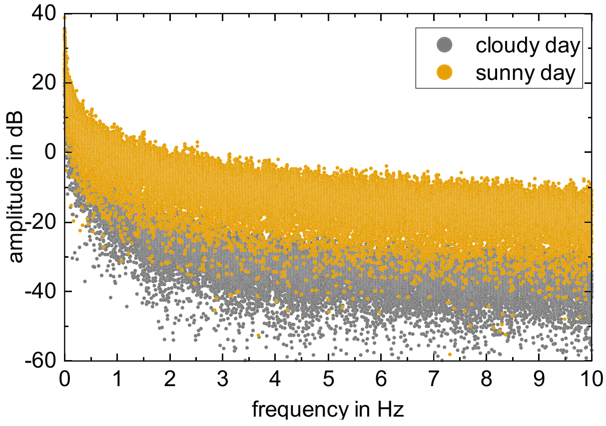

FIGURE 8 The frequency spectrum of the measured irradiance on the roof for the two test runs in autumn. Lower frequencies dominate, the amplitude decreases continuously with higher frequencies. This behavior is more distinct on the cloudy day, while on the sunny day the decrease is slower. 98.8% of the irradiance occur below 5 Hz on the cloudy day (98.1% for the sunny day respectively)

We performed an FFT high pass filtering, that cuts off static and low frequency transient irradiance, with different cut-off frequencies ranging from 0.002 to 200 Hz to determine the percentage of the irradiance that occur at higher frequencies. In practice this cut-off frequency could be the maximum working frequency of a maximum power point tracker for example. Above that frequency the maximum power point of a solar module would not be tracked properly. Figure 9A–F shows the relative irradiance that occurs above certain cut-off frequencies for the different seasons, street types and weather conditions. The individual symbols indicate the signal energy (integral of the square magnitude) of the filtered signal normalized to the unfiltered signal. Values are shown separately for the roof sensor and the mean of the left and right sensor. Note that most of the irradiance occur at even lower frequencies, that cannot be shown here due to limited computational accuracy (the resolution in frequency domain of the FFT is about 0.001 Hz here, depending on the data size). Toward 0 Hz cut-off frequency (not visible here because of logarithmic scale) the relative irradiance must of course be 100% for all plots as no frequencies are filtered out.

In Figure 9A one can see that in autumn, for sunny weather, irradiance changes at higher frequencies are more prominent than for cloudy weather. The reason for that is likely the more diffuse light when cloudy, which causes more soft shadows as described earlier. Frequencies above 10 Hz are pretty much negligible for both cases though. The influence of the street types is less significant as that of the weather. But we see that higher frequencies occur more often for "wide streets fast" than for "wide streets slow" and less often for "narrow streets." Apparently, the higher driving speed on the wider streets lead to more high frequency irradiance changes. Also the difference between street types is smaller for cloudy weather here, as "narrow streets" and "wide streets slow" barely show any difference. We also see that frequencies above 1 Hz contribute less than 2% to the overall energy and frequencies above 10 Hz are virtually irrelevant. For the side-looking sensors (see Figure 9B) the general behavior is very similar to what we find for the roof sensor. Nevertheless we see overall higher frequencies here. For cloudy weather on "wide streets fast," 2% of the energy occurs at frequencies above 100 Hz. As the probability to be shaded is higher for the sides,[13] consequently there are also more often transitions from shaded to non-shaded situations or vice versa.

In winter (Figure 9C) we see a similar behavior as in autumn regarding the weather conditions, but even more distinct. There are even more higher frequencies for sunny and less for cloudy weather. Also, for sunny conditions, higher frequencies are more often found for "wide streets fast," with still 2% above 100 Hz. On the other hand for cloudy weather there are virtually no differences between street types at all and even the lowest frequencies are very insignificant. Due to the very low base irradiance and the purely diffuse light, there are very little changes measured at all. For the side-looking sensor (Figure 9D) we see more higher frequencies especially for cloudy weather. Also for cloudy weather the influence of the street types is higher than for the roof sensors particularly for higher frequencies, as "wide streets slow" show relative signal energy of almost 7% above 100 Hz. The lower solar altitude in winter causes longer shadows. So the probability that shadows from smaller objects are cast on the street is higher as for higher solar altitudes. Therefore more irradiance changes occur on the car body.

In summer the behavior is quite the opposite of what we find in winter: The difference between sunny and cloudy weather becomes less significant for the measurements on the roof (Figure 9E). It is similar to the difference between the street types. Frequencies above 1 Hz are only relevant on "wide streets fast" and frequencies above 100 Hz only for cloudy weather. For the side-looking sensors we find a similar behavior as for the other seasons (Figure 9F), with overall higher frequencies. The influence of the street types is significant here. For cloudy weather "wide streets fast" show the highest frequencies observed in all test runs with more than 10% of the irradiance occurring above 100 Hz. Also the "wide streets slow" sections show more than 3% of the irradiance at more than 100 Hz.

5 | CONCLUSION

We assembled a test setup to measure the incident irradiance onto a car body while driving. The test setup allows to measure the irradiance on the roof and on the left and right sides with high time resolution. In six test runs we investigated the influence of different environmental conditions (season, weather, foliation, and different street types) on the amount of the incident irradiance and on the frequency spectrum in which irradiance changes occur. For the time averaged irradiance we find the weather conditions to more crucial than the season, as the lowest as well as the highest average values where measured in summer. Due to the lower maximum irradiance the influence of the weather is less significant in autumn and almost negligible in winter though. The influence of the street types turns

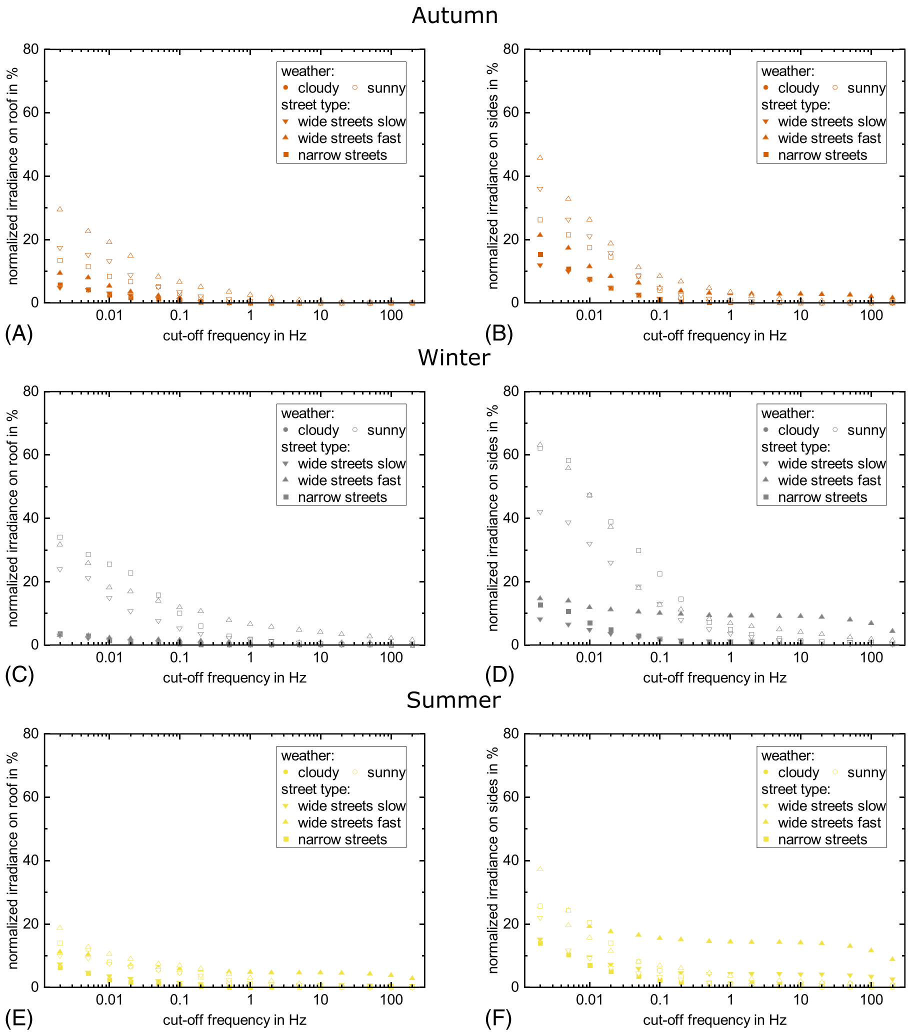

FIGURE 9 Normalized spectral density over high pass filter cut-off frequency. The plots show the part of the transient irradiance that occurs above certain frequencies. The vertical axis shows the integral of the square magnitude of the high pass filtered sensor signals normalized to the unfiltered signals. The plots on the left (A), (C), and (E) show the values for the roof sensor and the plots on the right (B), (D), and (F) show the values for the side-looking sensors (mean of left and right) for autumn, winter, and summer, respectively

out to be quite inconsistent and depends itself on the weather and season. The average measured irradiance on the sides is 43.1% of the average irradiance on the roof. The deviation from that value is small for most of the test runs. Only under sunny conditions in winter where it is substantially higher (up to 92%) and in summer where it is noticeably lower (down to 26%), the variation is significant. Due to the more diffuse light under cloudy conditions, the side-to-roof ratio vary barely. The influence of the street types more systematic here as the side-to-roof ratio is always lower on narrow streets while the wider street types differ very little.

We also investigated the transient behavior of the irradiance with high time resolution. By high-pass filtering we find that most of the incident irradiance occur at low frequencies, mostly below 1 Hz. Although in certain situations irradiance changes can occur at frequencies of even more than 100 Hz. The influence of the weather conditions on the frequency spectrum in turn is influenced by the season. In autumn sunny conditions cause slightly higher frequencies, while in winter the difference is significantly higher and in summer almost negligible. The street types have a smaller impact on the frequency spectrum than the weather conditions and for most test runs we see the highest frequencies for “wide streets fast.” Hence, we infer that the driving speed has a higher influence on the frequency of irradiance changes than other factors like the probability of shading or reflections by objects. Through out the test runs we find a higher amount of irradiance occurring at higher frequencies on the sides. Likely due to the higher probability for the sides to be shaded by objects resulting in more dark-light and light-dark transitions.

From the results of the frequency analysis we can state that for most situations a maximum power point tracking frequency of 1 Hz would be sufficient to follow the occurring irradiance changes. There are situations though that require a significantly higher tracking frequency of 100 Hz or more to achieve an optimum energy conversion efficiency. Still tracking frequencies that high might not be required to achieve the maximum energy harvesting possible, as the PV-system would not necessarily operate far off its maximum power point between adjustments. Even though it might be advantageous to use a low pass filtering at MPPT input to avoid aliasing, as high frequency illumination changes cannot entirely be excluded.

ACKNOWLEDGEMENTS

We like to thank Hartmut Schwarz from MBE for providing and driving the car, Leonardo Mörlein from the Institute of Microwave and Wireless Systems of the Leibniz University Hannover for counsel on signal processing and the Bundesministerium für Wirtschaft und Energie (BMWi) for funding under grant no. 0324275F. Open Access funding enabled and organized by Projekt DEAL.

DATA AVAILABILITY STATEMENT

The data that support the findings of this study are available from the corresponding author upon reasonable request.

ORCID

Gustav Wetzel https://orcid.org/0000-0001-5521-6085
Jan Krügener https://orcid.org/0000-0001-7095-9768
Dennis Bredemeier https://orcid.org/0000-0002-1733-4512
Robby Peibst https://orcid.org/0000-0001-8769-9392

REFERENCES

1. Richardson DB. Electric vehicles and the electric grid: a review of modeling approaches, Impacts, and renewable energy integration. *Renew Sustain Energy Rev*. 2013;19(C):247-254.
2. Filote C, Felseghi R-A, Raboaca MS, Aşchilean I. Environmental impact assessment of green energy systems for power supply of electric vehicle charging station. *Int J Energy Res*. 2020;44(13):10,471-10,494.
3. Kanz O, Reinders A, May J, Ding K. Environmental impacts of integrated photovoltaic modules in light utility electric vehicles. *Energies*. 2020;13(19):5120.
4. Abdelhamid M, Singh R, Qattawi A, Omar M, Haque I. Evaluation of on-board photovoltaic modules options for electric vehicles. *IEEE J Photovoltaics*. 2014;4(6):1576-1584.
5. Sierra Rodriguez A, de Santana T, MacGill I, Ekins-Daukes NJ, Reinders A. A feasibility study of solar pv-powered electric cars using an interdisciplinary modeling approach for the electricity balance, co2 emissions, and economic aspects: the cases of the netherlands, norway, brazil, and australia. *Prog Photovolt Res Appl*. 2020;28(6):517-532.
6. Araki K, Ji L, Kelly G, Yamaguchi M. To do list for research and development and international standardization to achieve the goal of running a majority of electric vehicles on solar energy. *Coatings*. 2018;8(7):251.
7. Araki K, Ji L, Kelly G, others. Modeling and standardization researches and discussions of the car-roof pv through international web meetings. In: 2019 IEEE 46th Photovoltaic Specialists Conference (PVSC); 2019; Chicago, IL, USA:2722-2729.
8. Wetzel G, Salomon L, Krügener J, Peibst R. Specifications for maximum power point tracking in vehicle-integrated photovoltaics based on high-resolution transient irradiance measurements. In: 2020 47th IEEE Photovoltaic Specialists Conference (PVSC); 2020:1124-1126.
9. Department of geo information cityofHanover(Germany). Open GEOData, Stadtmodell Hannover CityGML LoD2. Licensed under CC-BY-4.0 - Bereich Geoinformation - LH Hannover. Accessed October 11, 2021. https://www.hannover.de/Leben-in-der-Region-Hannover/Verwaltungen-Kommunen/Die-Verwaltung-der-Landeshauptstadt-Hannover/Dezernate-und-Fachbereiche-der-LHH/Stadtentwicklung-und-Bauen/Fachbereich-Planen-und-Stadtentwicklung/Geoinformation/Open-GeoData
10. © 2019 Google Google. Google Earth Pro. Imagery date 4 January 2019.
11. Institute of Meteorology and Climatology Leibniz University Hannover. Weather Archive. Accessed October 6, 2021. https://www1.muk.uni-hannover.de/hp-design2020/weather_archive_frame_en.html
12. Suncalc.org © Thorsten Hoffmann. Suncalc. https://www.suncalc.org/#/52.3723,_9.7382,_11/2020.06.24/13:04/1/3; 2020.
13. Araki K, Ota Y, Masuda T, Sato D, Yamaguchi M. Solar irradiance onto car body using mobile multiple pyranometer array system for vehicle-integrated photovoltaic applications—measurement a modeling. In: Pvsec-29 proceeding; 2019:2592-2598.
14. Ota Y, Araki K, Yamaguchi M. Estimation of the angular distribution of solar irradiance onto the vehicle using shading model. In: Pvsec-29 Proceeding; 2019:1124-1126. https://doi.org/10.1109/PVSC45281.2020.9300565

How to cite this article: Wetzel G, Salomon L, Krügener J, Bredemeier D, Peibst R. High time resolution measurement of solar irradiance onto driving car body for vehicle integrated photovoltaics. *Prog Photovolt Res Appl*. 2022;30(5):543-551. doi:10.1002/pip.3526